Title
EFFECT OF CHLORIDES ON Na2SO4-INDUCED HOT CORROSION OF MCrAl's

Authors
Misra, A.K.
Whittle, D.P.

Publication Date
1982-04-01

LBL-14388
Preprint

Lawrence Berkeley Laboratory
UNIVERSITY OF CALIFORNIA

Materials & Molecular
Research Division

Submitted to Corrosion Science

EFFECT OF CHLORIDES ON Na_2SO_4-INDUCED HOT CORROSION OF MCrAl's

A.K. Misra and D.P. Whittle

April 1982

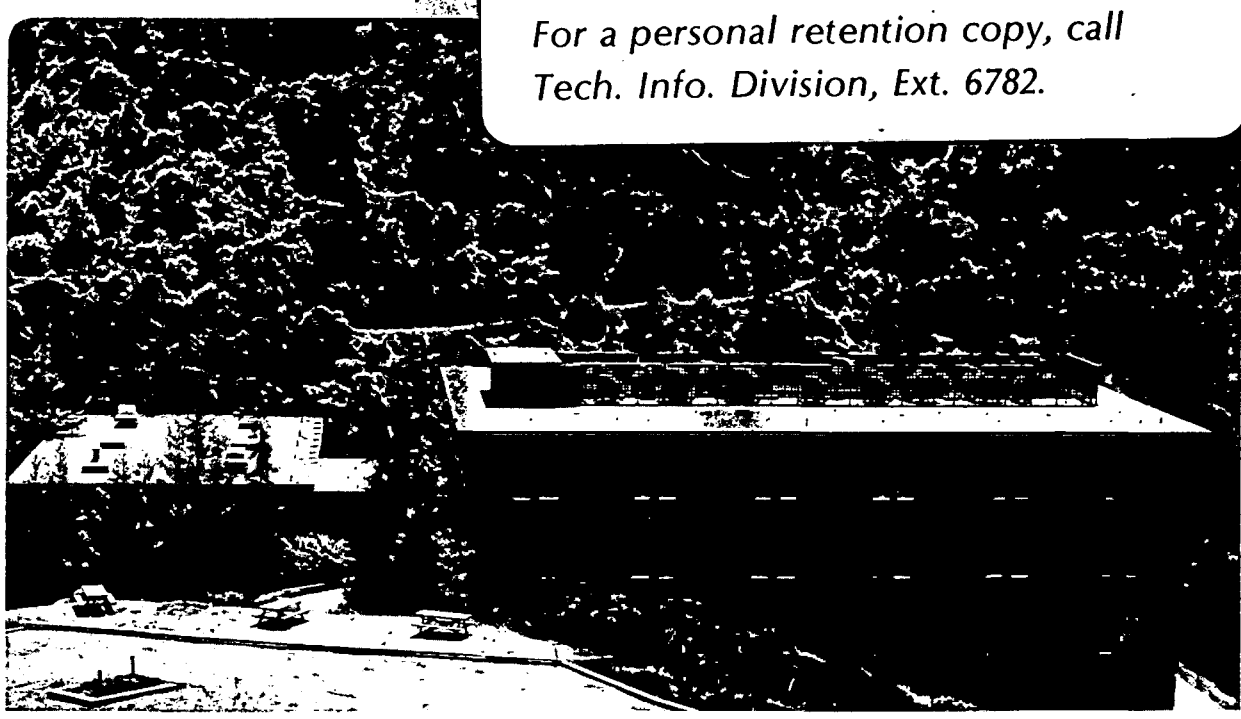

Prepared for the U.S. Department of Energy under Contract DE-AC03-76SF00098

DISCLAIMER

EFFECT OF CHLORIDES ON Na_2SO_4-INDUCED HOT CORROSION OF MCrAl's

A. K. Misra and D. P. Whittle

Lawrence Berkeley Laboratory
and Department of Materials Science and Mineral Engineering
University of California
Berkeley, California 94720

Acknowledgement - This work was supported by the Director, Office of Energy Research, Office of Basic Energy Sciences, Materials Sciences Division of the U.S. Department of Energy under Contract Number DE-AC03-76SF00098.

EFFECT OF CHLORIDES ON Na_2SO_4-INDUCED HOT CORROSION OF MCrAl's

ABSTRACT

The effects of HCl(g) and a Na_2SO_4-NaCl deposit on the hot corrosion behavior of Ni and Co-base alloys in the temperature range 750-850°C have been studied. Either chloride containing species enhances the preferential removal of Cr and/or Al (Al in preference to Cr in alloys containing both) from the alloy via formation of their respective chlorides at the oxide-metal interface. Condensed NaCl, in conjunction with Na_2SO_4, accelerates the process by generating Cl_2(g) at the oxide-melt interface due to sulfation of the chloride. Internal sulfidation is encouraged, and continued degradation occurs by a sulfidation-oxidation mechanism. Additions of Ti or Ce are suggested as a means for minimizing chloride-induced attack.

1. INTRODUCTION

Chloride containing species are often present in a typical gas turbine atmosphere. The major relevant species are NaCl(c), NaCl(g) and HCl(g)(l). The NaCl comes from sea-salt, ingested primarily as an aerosol along with the intake air. Thermodynamic calculations predict there should be complete conversion of NaCl to Na_2SO_4: however, some NaCl particles may remain, because of kinetic limitations. The upper limit of the partial pressure of NaCl(v), that can be attained, is of the order of 10^{-5} atm. and since this is lower than the equilibrium NaCl vapor corresponding to typical blade temperatures, vapor phase deposition on to the blade surface is highly unlikely. However, NaCl can deposit by direct impaction, and there are a number of theories

to account for this. The existance of NaCl particles on the blade surface is only likely to be transitory, since it can quickly evaporate; however, the residence time will increase with decreasing temperature.

The aggressiveness of condensed NaCl, in increasing the rate of Na_2SO_4 induced corrosion of alloys, has been demonstrated by several investigators in the recent past (2-4). Stringer et al. (2) studied the hot corrosion behavior of cobalt base alloys in the presence of a Na_2SO_4-NaCl deposit, and observed extensive grain boundary void formation and sulfidation for Co-25 Cr alloy at 900°C. Barkalow and Pettit (3) have studied the corrosion of CoCrAlY alloy in Na_2SO_4-NaCl mixture at 900°C and 649°C, and observed preferential removal of Al from the alloy; this was attributed to the formation of Al chlorides. However, the mechanism of formation of the Al chlorides was not clear, and needs further study. Similar observations for the preferential removal of Al were made by Jones (4). A maximum in corrosion rate at 750°C for IN 738, in the presence of a Na_2SO_4-NaCl deposit, was observed by McKee et al. (5), when the ambient atmosphere contained SO_2 along with O_2. The corrosion was attributed to the involvement of $Cl_2(g)$, generated by reaction of NaCl with SO_2 and O_2 in the ambient atmosphere.

The presence of NaCl(v) in the oxidizing atmosphere can also significantly affect the oxidation process. Breakdown of the protective oxide scale on alloys, such as low alloy steels, Ni-Cr alloys and stainless steels, has been demostrated by Hancock and his co-workers (6, 7), using a vibrational technique. Smeggil and Bornstein (8) have

shown that the presence of small amounts of NaCl(v) in the atmosphere substantially modifies the oxidation behavior of Ni-Al alloys at 900°C; this involves preferential removal of Al from the Al_2O_3 scale, and redeposition on the surface of the scale as whiskers. The presence of NaCl(g) also increases the spalling tendency of the protective oxides. Frequently, the higher rate of corrosion in the presence of NaCl(v) has been attributed to the formation of volatile chlorides by reaction of metals and alloys with NaCl, which causes considerable disruption of the protective oxide scale, thus, causing scale fracture. When alloys coated with Na_2SO_4 are exposed to an atmosphere containing NaCl(v), enhanced vaporization of Na_2SO_4 takes place (3, 9) by reaction of the Na_2SO_4(c) with HCl(g), generated from NaCl(v) reacting with trace amount of water vapor present in the atmosphere (10).

Since NaCl is converted to Na_2SO_4 and HCl(g) in a typical gas turbine atmosphere, the level of HCl(g) is higher than that of NaCl(v), and as a consequence, in the present investigation, HCl(g), not NaCl(v) has been assumed to be the predominant species.

The objectives of the present investigation are two fold: to study (1) the effect of condensed NaCl on the Na_2SO_4 induced corrosion behavior of Ni and Co base alloys; and (2) the effect of HCl(g) on the oxidation and Na_2SO_4 induced corrosion behavior of nickel and cobalt base alloys. The temperature range of interest is 750-850°C, which

corresponds to that of low power operation of gas turbines.

2. Experimental Procedure

The nominal composition of the alloys are given in Table I. All the alloys were prepared by vacuum melting and casting into 7x7x1.5 cm ingots, from which rectangular coupons, approximately 10x10x1 mm were cut. After annealing in vacuo at 950°C, the specimens were ground through 600 grit SiC papers and cleaned with alcohol and acetone before the start of an experiment.

The corrosion of alloys in the presence of a Na_2SO_4-NaCl deposit was carried out in a three zone temperature gradient furnace. The leading zone of the reaction furnace contains the salt reservoir (Na_2SO_4+NaCl) at a higher temperature than the final sample zone, while the intermediate zone ensures a suitable temperature gradient. Dry air, at a rate of 40cc/min., is passed through the furnace; salt vapor is picked up by the air stream, carried over the samples where it condenses. An Na_2SO_4-10 mole percent NaCl mixture was used and the salt generation section of the furnace kept at either 1000 or 1070°C. The vapor pressures over the salt mixture are unknown. Na_2SO_4 and NaCl at unit activity would have vapor pressures of $2x10^{-7}$ and $8.8x10^{-3}$ atm. respectively at 1000°C, and $2x10^{-6}$ and $2.1x10^{-2}$ atm. at 1070°C (1, 11). The vapor pressure of Na_2SO_4 is about 4 orders of magnitude lower than that of NaCl, and as a consequence, the salt deposit on the samples would be expected to be NaCl-rich. However, NaCl is

also known to accelerate the evaporation of Na_2SO_4 (3, 9), and indeed rapid evaporation of Na_2SO_4 was observed in the present experiments, the rate of evaporation increasing with temperature. In a preliminary experiment, a boat containing NaCl was placed in a cooler zone (600-800°C) of the furnace upstream from the salt zone, where its vapor pressure would be in the range of 10^{-6}-10^{-4} atm. This allowed a continuous flow of air + NaCl vapor to pass over molten Na_2SO_4 only, maintained at 1070°C: rapid evaporation of the sulfate was also observed. The details of the rapid evaporation of Na_2SO_4 in the presence of NaCl will be discussed in Appendix 1.

An inert (Pt) sample was used to determine the Na_2SO_4/NaCl ratio of the deposit after 100 hr exposure, which corresponds to a 4-5 mg/cm^2 deposit. (As with the later experiments the salt mixture was renewed every 8 hrs.) The deposit was chemically analyzed for $SO_4^=$ and $Cl^=$, and the results are shown in Table II. The Na_2SO_4/NaCl ratio increases with either an increase the salt zone or sample zone temperature.

For corrosion experiments, in which the effect of small amounts of HCl(g) or the corrosion behavior was studied, the HCl vapor was introduced into a reaction furnace by bubbling air through hydrochloric acid solution, maintained at constant temperature. The concentration of HCl(g) in the atmosphere was varied by changing the strength of the solution. For example, the partial pressure of HCl and H_2O in air, bubbled through an aqueous solution containing 20% HCl, are

6.31×10^{-4} and .025 atm. respectively at 20°C. By bubbling air through an aqueous solution containing HCl, very low levels of HCl could be introduced into the atmosphere. The gas turbine atmosphere also contains approximately 2% water vapor, thus, the atmosphere in the present experimental system is a good simulation. The corrosion experiments were performed in a simple furnace maintained at a constant temperature. The samples were placed inside an alumina boat. In the present investigation, the effect of small amount of HCl(g) on corrosion of alloys was studied both with and without the presence of a Na_2SO_4 deposit on the sample. For corrosion experiments in the presence of a Na_2SO_4 deposit, the samples were coated with Na_2SO_4, by spraying an aqueous solution of Na_2SO_4 on the sample, heated to 200-300°C.

Accelerated corrosion tests were also performed in which the alloys were subjected to cyclic testing at the reaction temperature. Each cycle consisted of 24 hr. at temperature, followed by cooling to room temperature for 1 hr. and then repeat of the cycle upto a maximum of seven times. This gives a maximum exposure of 168 hours.

Selected samples of the corroded alloys were examined by conventional metallographic and SEM techniques. EPMA and/or EDAX analysis were also carried out. No kinetic measurements were undertaken.

3. Corrosion of Alloys in the Presence of Na_2SO_4-NaCl Deposit

Results

The corrosion morphology of nickel and cobalt base

alloys are similar in nature; one or other is described.

a. Binary M-25 Cr (M=CoCrNi) Alloys:

The Na_2SO_4-NaCl phase diagram (12) shows a eutectic at 602°C with no terminal solid solutions. All the compositions in Table II are in the molten region of the Na_2SO_4-NaCl phase diagram; corrosion always takes place in the presence of a melt.

The oxides formed beneath the melt are highly porous, containing numerous cracks and holes as shown in Figure 1. The melt can be seen penetrating through the cracks and holes. The scale morphology, for the corrosion of a binary Ni-25 Cr alloy at 750°C in the presence of a Na_2SO_4-NaCl deposit of high $NaCl/Na_2SO_4$ ratio, shows on outermost layer rich in S, Cl and Ni (Fig. 2), suggesting that this is a mixture of $NiO+Na_2SO_4+NaCl$. The NiO layer was formed during the transient stage of oxidation of the alloy and was subsequently penetrated by the melt. Beneath the outermost NiO layer, another thin layer of NiO is formed. However, the most significant feature of the morphology is a thin Cr-rich layer beneath the NiO layer. EPMA showed the presence of large amounts of chlorine inside the Cr rich scale, concentrating near the scale-metal interface. It appears that Cr chlorides are formed at this interface. A Cr depletion zone is also observed inside the alloy, adjacent to the scale-metal interface. Internal particles, which

look like voids, are also observed in the Cr depletion zone. A detailed analysis of the internal particles (Figure 3) shows them to be Cr chloride particles. Some of these Cr chloride particles are continuous and extend upto the scale-metal interface. Clearly, preferential removal of Cr from the alloy takes place to form a Cr chloride layer at the scale-metal interface, and this results in the Cr-depleted layer. After longer exposure times, the Cr depletion becomes more extensive and an internal porous zone, penetrating deep into the alloy, is observed (Figure 4). This zone contains several voids, which are not interconnected, and some fine sulfide particles. The outer scale in Figure 4 spalled at several locations, and is not visible in the figure.

With an increase in Na_2SO_4/NaCl ratio in the deposit, the scale morphology for corrosion of Ni 25 Cr at 750°C shows a sulfidation oxidation type of attack (Figure 5), which consists of a sulfidation front and an oxidation front inside the alloy. The sulfidation front penetrates ahead of the oxidation front. The sulfides are Cr-rich, containing small amounts of Ni. The scale morphology in Figure 5 also shows features that were observed for corrosion in the presence of a Na_2SO_4-NaCl deposit of high NaCl/Na_2SO_4 ratio: preferential removal of Cr from the alloy to form a Cr-rich

scale and void formation adjacent to the scale-metal interface. At 850°C, the Na_2SO_4/NaCl ratio in the deposit is higher than that of 750°C, and the scale morphology for corrosion of Ni-25 Cr alloy is similar to that of Figure 5, however, the extent of internal sulfidation is greater (Figure 6).

b. Ternary MCrAl (M=Co or Ni) Type Alloys:

A very thick scale is obtained for the corrosion of M 15 Cr 10 Al type alloys in the presence of Na_2SO_4-NaCl deposits of high NaCl/Na_2SO_4 ratio, although part of this usually spalls from the surface. Figure 7 shows a typical example. The scale comprises of (1) a thick external porous and layered scale; (2) an outermost part rich in the base metal (Co or Ni), but containing Cr, followed by a Cr-and Al-rich layer; (3) severe Al depletion in the alloy adjacent to the scale-metal interface; (4) large amounts of S and Cl at the scale-metal interface, suggesting the presence of a Na_2SO_4-NaCl melt. Examination of the scale-metal interface at a higher magnification (Figure 8) shows large numbers of pores inside the alloy adjacent to the interface, some of which are interconnected. In addition, a few cracks are observed in the internal porous region. The region in which the pores are present is depleted of Al and Cr, but enriched in

Cl and cobalt. These features suggest that the presence of the Na_2SO_4-NaCl deposit has promoted preferential removal of Al, and to a lesser extent Cr, from the alloy. This preferential removal increases the Co concentration at the scale-metal interface, to the extent that eventually a Co-rich scale can be formed. Repetition of this process, leads to a layered type of scale, consisting of alternate bands of Co-rich and Al+Cr rich scales. As with binary M-25 Cr alloys, increase in the Na_2SO_4/NaCl ratio of the deposit, increases the extent of internal sulfidation.

Discussion

The presence of NaCl, along with Na_2SO_4, in the deposit on the alloy surface affects the oxidation process by encouraging preferential removal of the alloying elements, Cr and Al, that are necessary to form a protective oxide. This appears to be via the formation of Cr and Al chlorides, both at the scale-metal interface and inside the alloy adjacent to the interface. A similar hypotheses, but via an internal network of pores, was proposed by Barkalow and Pettit (3) for the corrosion of CoCrAlY alloy in the presence of a NaCl-Na_2SO_4 deposit. Formation of Al chlorides took place inside the pores. However, they did not elaborate on the mechanism of formation of the chlorides.

Thus, to consider this further, it is instructive to examine the possible interaction of metals and alloys with the Na_2SO_4-NaCl mixture. Firstly, consider the direct reaction with liquid NaCl at 750°C. These can be expressed as

$$Ni(s)+2NaCl(\ell) = NiCl_2(s)+2Na(\ell) \quad [1]$$

$$K_{(1)\,750°C} = 3.6\times10^{-25} \quad [2]$$

$$Al(s)+3NaCl(\ell) = AlCl_3(\ell)+3Na(\ell) \quad [3]$$

$$K_{(3)\ 750°C} = 2.7\times10^{-27} \quad [4]$$

$$Cr(s)+NaCl(\ell) = CrCl_3(s)+3Na(\ell) \quad [5]$$

$$K_{(5)\ 750°C} = 9.5\times10^{-33} \quad [6]$$

$$Cr(s)+2NaCl(\ell) = CrCl_2(2)+2Na(\ell) \quad [7]$$

$$K_{(7)\ 750°C} = 9\times10^{-19} \quad [8]$$

The low values of the equilibrium constants point to the unliklihood of metal chlorides being formed by these direct reactions.

Oxidation of the alloy takes place beneath the Na_2SO_4-NaCl melt. From the Na-Ni-S-O stability diagram (see Figure 9), it can be seen that NiO is the primary product in the case of Ni. Although, Na-Al-S-O and Na-Cr-S-O diagrams have not been presented, both Al_2O_3 and Cr_2O_3 are more stable than NiO, and could also be formed beneath the melt. Reaction of these oxides with NaCl(ℓ) can be expressed as

$$NiO(s)+2NaCl(\ell) = NiCl_2(s)+Na_2O(\ell) \quad [9]$$

$$K_{(9)\ 750°C} = 4.7\times10^{-20} \quad [10]$$

$$Al_2O_3(s)+6NaCl(\ell) = 2AlCl_3(\ell)+3Na_2O(\ell) \quad [11]$$

$$K_{(11)\ 750°C} = 8.1\times10^{-75} \quad [12]$$

$$Cr_2O_3(s)+6NaCl(\ell) = 2CrCl_3(\ell) + 3Na_2O(\ell) \quad [13]$$

$$K_{(13)\ 750°C} = 5.4\times10^{-68} \quad [14]$$

Again, the direct reaction of the oxides with the NaCl component of the melt is not thermodynamically favorable.

The formation of oxides beneath the melt and the growth of the oxides require transport of oxygen through the melt. The solubility of O_2 in the melt is very low (13), and if the rate of transport of O_2 through the melt is less than the rate of oxidation, the oxygen will be supplied from oxide ions in the melt. In the melt containing Na_2SO_4, the Na_2O activity and P_{SO_3} are related by the equilibrium conditions for the reaction:

$$Na_2SO_4(\ell) = Na_2O(\ell)+SO_3(g) \quad [15]$$

$$K_{15} = \frac{a^L_{Na_2O}\ P_{SO_3}}{a^L_{Na_2SO_4}} \quad [16]$$

Thus, a decrease in oxidation activity (a_{Na_2O}), due to the consumption of oxide ion, increases the P_{SO_3} at the oxide-melt interface. In addition, due to the low solubility of O_2 in the melt, the P_{O_2} at the melt-oxide interface is low and some of the SO_3 will decompose to SO_2 via the raction

$$SO_3 \rightarrow SO_2 + \tfrac{1}{2}\ O_2 \quad [17]$$

to maintain the SO_3-O_2-SO_2 equilibrium. Increase in the P_{SO_3} at the oxide-melt interface, due to the de-

crease in oxide ion activity, leads to sulfation of the NaCl component of the melt via the reaction.

$$2NaCl(\ell)+SO_3+\frac{1}{2}O_2 = Na_2SO_4(\ell)+Cl_2(g) \quad [18]$$

and generates $Cl_2(g)$ at the oxide-melt interface. The stability diagrams for Ni-Cl-O, Cr-Cl-O and Al-Cl-O (Figures 10-12) indicate that chlorides of the alloy components can be formed at low oxygen potentials. Thus, if $Cl_2(g)$ can diffuse to the oxide-metal interface, where the oxygen potential is low, the metal chloride can be formed. Diffusion of the second oxidant (sulfur, nitrogen) in atmospheres containing oxygen have been observed for oxidation of metals and alloys in O_2+SO_2 and O_2+N_2 mixtures (14), although the mechanism of diffusion through the oxide is still debatable. For oxidation of Si in an atmosphere containing O_2+Cl_2, the Cl concentration in the SiO_2 is known to increase gradually from the oxide-gas interface to the oxide-metal interface (15). It is proposed that in a similar manner Cl_2 diffuses through the oxides, formed on these alloys, forming metal chlorides at the oxide-metal interface. For binary M-25Cr alloys, thermodynamic factors favor the formation of Cr chlorides, whereas for the ternary alloys, Al chlorides are thermodynamically favored.

Formation of Al and Cr chlorides at the oxide-metal interface depletes the alloy of Al and Cr. Thus, internal chloride particles can be formed in the depleted region, where the concentration of the alloying

elements is not high enough to form a continuous layer of chloride at the oxide-metal interface: the presence of internal Cr chloride particles in Figure 3 confirms this. The vapor pressures of $CrCl_2$ and $AlCl_3$ are high at elevated temperatures. For example, the equilibrium vapor pressure of $CrCl_2(s)$ at 750°C is $3x10^{-4}$ atm., and that of $AlCl_3(\ell)$ at 750°C is 32 atmospheres. Thus, formation of internal $AlCl_3(\ell)$ creates a high pressure inside the alloy, which might open cracks in the vicinity of the internal chloride particles. This crack formation leads to a continuous network of pores through which Al chloride vapor is transported to the outer surface. At the outer surface, where the oxygen potential is high, the Al chloride vapor is converted to Al_2O_3. Melt is also able to penetrate through the continuous network of pores. The high vapor pressure of $AlCl_3$, makes it readily transportable to the outer surface, and Al is rarely detected in the internal porous zone. In contrast, the equilibrium vapor pressure of $CrCl_2$ at 750°C is much lower, and accordingly the rate of removal of $CrCl_2$, either from the scale-metal interface or from the internal chloride particles, is much slower. Thus, EPMA does detect Cr chlorides, at the interface and within the alloy.

When one element of the alloy is preferentially removed from the alloy and the rate of diffusion of the alloying element from inside of the alloy is slow, extensive internal porosity can develop inside the

alloy. The details of this process have been described by Harrison and Wagner (16). At lower temperatures (∿750°C), the rate of diffusion within the alloy is slow, and thus, the preferential removal of Al and Cr as chlorides creates extensive porosity. This was shown for a Ni-25 Cr alloy in Figure 4.

When oxidation of alloys takes place beneath a Na_2SO_4-NaCl melt, formation of internal sulfides is also observed. The extent of internal sulfidation is dependent on the Na_2SO_4/NaCl ratio of the deposit. This can be explained as follows. As indicated earlier, due to the formation of the metal oxide, the Na_2O activity of the melt at the scale-melt interface decreases with a corresponding increase in the equilibrium SO_3 partial pressure at the oxide-melt interface. This SO_3 causes sulfation of the NaCl(ℓ), generating Cl_2(g). However, the sulfation reaction also requires O_2, and this comes from the decomposition of SO_3 to maintain the SO_3-O_2-SO_2 equilibrium. Thus, from stoichiometry considerations of reactions 17 and 18, two moles of NaCl consume one mole of SO_3; and one mole of SO_2 is not consumed. The pressure of SO_2 in the atmosphere is known to enhance internal sulfide formation (14). For a melt with high Na_2SO_4/NaCl ratio, the total amount of NaCl is low, and all the generated SO_3+SO_2 is not consumed in NaCl sulfation. Thus, increased internal sulfidation can be expected for oxidation beneath a Na_2SO_4-NaCl deposit of high Na_2SO_4/NaCl

ratio. The internal sulfidation process is further accelerated by the severe Al and Cr depletion produced at the alloy surface by formation of volatile chlorides in the manner described earlier. Once the internal sulfides are formed, further degradation continues via a sulfidation-oxidation mechanism (49, 50).

4. Influence of HCl(g) on the Corrosion Behavior: Results and Discussion

Influence of HCl(g) on the Oxidation of Alloys

The presence of small amount of HCl(g) in the atmosphere produces a porous scale, which is usually cracked and spalled at several places. Figure 13 shows the top surface of the scale on Ni-25Cr oxidized for 1 hr in an atmosphere consisting of a mixture of air, water vapor and HCl; the partial pressure of HCl is 6.31×10^{-4} atm. and that of water vapor is .025 atm. The top surface of the scale appears to be highly porous and several large holes are also observed in the scale surface. The scale is primarily Cr_2O_3. No chloride containing species could be detected on the surface. The cross-section of a similar sample shows a thin Cr_2O_3 scale detached from the surface and few internal voids inside the alloy adjacent to the scale-metal interface (Figure 14).

In an atmosphere containing small amounts of HCl(g), the addition of only 2.5 wt.% Al to the Ni-25Cr alloy promotes the formation of an external Al_2O_3 scale,

shown in Figure 15. Few internal oxide particles or voids are observed near the scale-metal interface. Extensive EPMA did not show the presence of chlorine, either inside the scale or at the scale-metal interface. A continuous Al_2O_3 scale along with some internal oxide particles and voids was also observed for alloys containing higher amount of Al, e.g., Ni 15Cr 10Al; this is shown in Figure 16. An Al depletion next to the scale-metal interface is also evident.

In another publication (19), it has been shown that at temperatures of the order of 750°C, oxidation of Ni-Cr alloys in air yielded a very thin scale, which could not be examined by optical metallography. Oxidation of ternary Ni-Cr-Al alloys in air also gives similar results. In addition, preferential formation of the more stable oxides (Cr_2O_3 and Al_2O_3) did not occur even after extended periods of oxidation. However, somewhat surprisingly, addition of HCl(g) to the oxidizing atmosphere has promoted preferential oxidation of the stable oxide forming components. Even a Ni-25Cr alloy containing 2.5 wt.% Al forms a continuous layer of Al_2O_3. This must be related to the formation of Al and Cr chlorides at the oxide-metal interface and subsequent transformation of these chlorides into oxides at the oxide-gas interface, even though, no Cl is detected in the scale. The less severe environment, when a chloride containing deposit is absent, probably means that the level of chlorine

in the oxide and at the oxide-metal interface are too low to be detected with the present techique (EPMA). Meek (20) studying the oxidation of Si in an atmosphere containing 1% HCl in O_2, detected traces of Cl in the oxide scale using a nuclear backscattering spectrometry technique.

Effect of HCl(g) on the Na_2SO_4 Induced Corrosion Behavior of Alloys

The reaction of HCl(g) with Na_2SO_4 can be described by the reaction

$$Na_2SO_4(c)+2HCl(g) = 2NaCl(c)+SO_3(g)+H_2O(g) \qquad [19]$$

$$K_{19} = \frac{(a_{NaCl})^2 \, P_{SO_3} \, P_{H_2}}{a_{Na_2SO_4} \cdot (P_{HCl})^2} \qquad [20]$$

In the experimental arrangement used, air is continuously bubbled through an aqueous solution containing HCl, before entering the reaction furnace, and thus, the P_{HCl} and P_{H_2O} in the atmosphere are fixed. Thus, assuming ideal solution behavior between Na_2SO_4 and NaCl in the melt, the equilibrium $a_{Na_2SO_4}$ and a_{NaCl} for a given initial amount of Na_2SO_4 deposit can be calculated from stoichiometric considerations and equation 20. For an initial deposit of Na_2SO_4 equal to 2 mg, and when the P_{HCl} and P_{H_2O} in the atmosphere are 6.31×10^{-4} atm. and .025 atm. respectively, calculations show that at equilibrium, the activity of Na_2SO_4 and NaCl are .877 and .123 respectively. The equilibrium P_{SO_3} is calculated to be 9.25×10^{-7} atm. Experiments

in the present investigation were carried out in a continuous flow, and thus, the SO_3 generated can be swept away, requiring more Na_2SO_4 to react with HCl(g). Thus, the deposit is gradually converted to a melt of high $NaCl/Na_2SO_4$ ratio. The scale morphology for corrosion of alloys coated with Na_2SO_4 and exposed to an atmosphere containing 600 ppm HCl in air shows all the characteristic features of the morphology for corrosion in Na_2SO_4-NaCl mixture (Figure 17).

5. Summary and Concluding Remarks

The effects of HCl(g) and Na_2SO_4-NaCl deposit on the corrosion behavior of Ni and Co base alloys have been studied in the temperature range 750-850°C, and the major conclusions are summarized below:

(1) The presence of any of the chlorine containing species affects the corrosion behavior by preferential removal of Cr and Al from the alloy. Thermodynamic factors favor the preferential removal of Al from alloys containing both elements.

(2) Preferential removal of Al and Cr from the alloy occurs via the formation of their respective chlorides at the oxide-metal interface by diffusion of Cl to this location.

(3) The presence of condensed NaCl along with Na_2SO_4 and the alloy surface accelerates the preferential removal of Al and Cr from the alloy by generating $Cl_2(g)$ at the oxide-melt interface due to the sulfation of NaCl.

(4) For a deposit of high Na_2SO_4/NaCl ratio, preferential removal of Al and Cr from the alloy facilitates the formation of internal sulfides and continued degradation occurs by a sulfidation-oxidation mechanism.

In the present investigation, the corrosion experiments are carried out under very severe conditions: for example, the level of HCl(g) and the amount of Na_2SO_4-NaCl deposit are much higher than would occur under actual turbine operating conditions. Nevertheless, it is clear that the major role of the chlorine containing species is to preferentially remove Al and Cr from the alloy. It is encouraging to note that small Al addition (2.5 wt.%) to binary Ni-25Cr alloy lead to preferential removal of Al only; Cr is not selectively removed. This gives an important suggestion in regards to the development of alloys or coatings resistant to chlorine attack. The preferential removal of the alloying element is believed to take place by formation of chlorides at the oxide-metal interface and this can be prevented for the desired alloying element by adding small quantity of another element whose chlorides are more stable. For a binary Ni-25 Cr alloy, this was accomplished by adding small amount of Al. Besides Al, Ti and Ce are also possibilities. For example, at the P_{O_2} level corresponding to the Cr-Cr_2O_3 interface, the P_{Cl_2} required for formation of Cr Cl_2 at until activity is calculated to be 1.72×10^{-14} atm. at 750°C, and at the P_{O_2} level corresponding to the Ti-TiO interface, the P_{Cl_2} required for formation of $TiCl_4$(v) at 1 atmosphere at 750°C is 7.78×10^{-17} atm, which is 3 orders

of magnitude lower than that required for formation of $CrCl_2$ at the $Cr-Cr_2O_3$ interface. Similarly at 750°C, the P_{Cl_2} required for formation of $CeCl_3$ at unit activity at the $Ce-CeO_2$ interface is 2.103×10^{-28} atm., which is 14 orders of magnitude lower than that required for formation of $CrCl_2$ at unit activity at the $Cr-Cr_2O_3$ interface.

For ternary alloys containing Al, the choices for additional elements are limited because of the very low P_{Cl_2} (1.26×10^{-18} atm.) required for formation of $AlCl_3(v)$ at one atm. pressure at 750°C at the $Al-Al_2O_3$ interface. The only choices for the ternary alloys are reactive elements like cerium.

ACKNOWLEDGEMENTS

This research was supported by the Director, Office of Energy Research, Office of Basic Energy Sciences, Materials Sciences Division of the U.S. Department of Energy under Contract Number DE-AC03-76SF00098. The work was completed in partial fulfilment for one of us (AKM) of the requirements for the degree of Ph.D. of the University of California.

REFERENCES

1. F. J. Kohl, C. A. Stearns and G. C. Fryburg in "Metal-Slag-Gas Reactions and Processes," edited by Z. A. Foroulis and W. W. Smeltzer, Electrochem. Soc., Princeton, N. J. (1975) p. 649.

2. J. Stringer, V. Najarajan and D. P. Whittle in "High Temp. Metal Halide Chemistry," edited by D. L. Hildenbrand and D. D. Cubicciotti, the Electrochem. Soc., Princeton, N.J. (1978), p. 509.

3. R. H. Barkalow and F. S. Pettit, ibid, p. 617.

4. K. H. Stern and R. L. Jones, ibid, p. 608.

5. D. W. McKee, D. A. Shores and K. L. Luthra, J. Electrochem. Soc., 125, 411 (1978).

6. P. Hancock, R. C. Hurst and A. R. Sollars in "Chemical Metallurgy of Iron and Steel," Special Publication, Iron and Steel Institute, (1973) p. 413.

7. R. C. Hurst, J. B. Johnson, M. Davies and P. Hancock in "Proc. C.E.G.B. Conf. on Corrosion and Deposition in Gas Turbines," London, Dec. 1972, edited by A. B. Hart and A. J. B. Cutler, p. 143.

8. J. G. Smeggil and N. S. Bornstein, J. Electrochem. Soc., 125, 1283 (1978).

9. R. J. Jones and S. T. Gadomski, ibid, 124, 1641 (1977).

10. C. A. Stearns, F. J. Kohl, G. C. Fryburg and R. A. Miller in "High Temp. Metal Halide Chemistry," edited by D. L. Hildenbrand and D. D. Cubiccioti, Electrochem. Soc., Princeton, N. J. (1978) p. 555.

11. I. Barin and O. Knacke, "Thermochemical Properties of Inorganic Substances," Springer Verlag (1973).

12. P. I. Fedorov and K. A. Bol'shakov, Zhur. Neorg. Khim., 4, 893 (1959).

13. R. E. Andersen, J. Electrochem. Socl, 126, 328 (1979).

14. C. S. Giggins and F. S. Pettit, Oxidation of Metals, 14, 363 (1980).

15. P. I. Fedorov and K. A. Bol'shakov, Zhur. Neorg. Khim. 4, 893 (1959)

16. Y. J. Van der Meulen, C. M. Osburn, and J. F. Ziegler, J. Electrochem. Socl, 122, 284 (1975).

17. C. J. Spengler and R. Viswanathan, Metall. Trans., 3, 161 (1972).

18. M. E. El Dahshan, D. P. Whittle and J. Stringer, Oxidation of Metals, 8, 179 (1974).

19. A. K. Misra and D. P. Whittle, to be published.

20. R. L. Meek, J. Electrochem. Soc., 120, 308 (1973).

TABLE I

Nominal Composition of Alloys in the Studies on Effect of Chloride Containing Species on Na_2SO_4 Induced Corrosion Behavior of Alloys (all compositions are in weight percent)

Ni-25 Cr	Co-25 Cr
Ni-25 Cr 2.5 Al	Co-25 Cr 2.5 Al
Ni-15 Cr 10 Al	Co-15 Cr 10 Al

TABLE II

Na_2SO_4/NaCl Ratio on an Inert Sample as a Function of Salt Zone and Sample Temperature

Salt Zone Temperature	Sample Temperature	Mole Fraction of Na_2SO_4 $x_{Na_2SO_4}$	Mole Fraction of NaCl x_{NaCl}
1070	850	.84	.16
	750	.43	.57
1000	850	.38	.62
	750	.19	.81

FIGURE CAPTIONS

1. Scanning electron image of the surface of the scale of Ni-25 Cr corroded in the presence of a Na_2SO_4-NaCl melt for 5 hours.

2. Scanning electron image and x-ray distribution for Ni-25 Cr, corroded in the presence of a Na_2SO_4-NaCl melt of high $NaCl/Na_2SO_4$ ratio, for 4, 24 hr. cycles at 750°C (salt zone temperature - 1000°C).

3. Scanning electron image and x-ray distribution for the internal particles of Figure 38.

4. Cross-section of Ni-25 Cr, corroded, in the presence of a Na_2SO_4-NaCl melt of high $NaCl/Na_2SO_4$ ratio, for 7, 24 hr. cycles at 750°C (salt zone temperature 1000°C).

5. Cross-section of Ni-25 Cr, corroded in the presence of a Na_2SO_4-NaCl melt of high $Na_2SO_4/NaCl$ ratio, for 5, 24 hr. cycles at 750°C (salt zone temperature 1070°C).

6. Cross-section of Ni-25 Cr, corroded in the presence of a Na_2SO_4-NaCl melt of high $Na_2SO_4/NaCl$ ratio for 5, 24 hr. cycles at 850°C (salt zone temperature 1070°C).

7. Scanning electron image and x-ray distribution for Co 15 Cr 10 Al, corroded in the presence of a Na_2SO_4-NaCl melt of high $NaCl/Na_2SO_4$ ratio for 7, 24 hr. cycles at 750°C (salt zone temperature - 1000°C).

8. Scanning electron image and x-ray distribution for the interface in Figure 43.

9. Na-Ni-S-O stability diagram at 750°C.

10. Ni-Cl-O stability diagram at 750°C.

11. Cr-Cl-O stability diagram at 750°C.

12. Al-Cl-O stability diagram at 750°C.

13. Scanning electron image of the surface of Ni-25 Cr oxidized at 750°C in an atmosphere containing 600 ppm HCl in Air for 1 hour.

14. Cross-section of Ni-25 Cr, oxidized at 750°C in an atmosphere containing 660 ppm HCl in air for 6 hours.

15. Cross-section of Ni-25 Cr 2.5 Al, oxidized at 750°C in an atmosphere containing 600 ppm HCl in Air for 3, 24 hour cycles.

16. Cross-section of Ni 15 Cr 10 Al, oxidized at 750°C in an atmosphere containing 600 ppm HCl in Air for 5, 24 hour cycles.

17. Cross-section of Ni-25 Cr, coated with 1.5 mg/cm^2 Na_2SO_4 and oxidized at 750°C in an atmosphere containing 600 ppm HCl in air for 48 hours.

APPENDIX 1

ENHANCED VAPORIZATION OF Na_2SO_4 IN THE PRESENCE OF NaCl

Consider the experimental system of Barkalow and Pettit[1] and Jones et.al.[2] in which 300 ppm of NaCl vapor was passed over Na_2SO_4 at 900°C. For a vapor pressure of NaCl of $3x10^{-4}$ atm. above the Na_2SO_4 melt, the equilibrium activity of NaCl in the melt is 0.156, and that of Na_2SO_4 is 0.844. Now the P_{Cl_2} in the atmosphere is governed by the equilibrium conditions for the reaction

$$2NaCl(\ell)+\tfrac{1}{2}O_2 = Na_2O(\ell)+Cl_2(g) \qquad [1]$$

$$K_{1(900°C)} = 6.79x10^{-17} = \frac{a_{Na_2O} \cdot P_{Cl_2}}{(a_{NaCl})^2 (P_{O_2})^{\frac{1}{2}}} \qquad [2]$$

For $a_{NaCl} = .156$, $P_{O_2} = .21$ atm., and assuming stoichiometric decomposition, the P_{Cl_2} in the atmosphere is calculated to be $8.372x10^{-10}$ atm. Similarly, the SO_3 partial pressure in the atmosphere is governed by the reaction

$$Na_2SO_4(\ell) = Na_2O(\ell)+SO_3(g) \qquad [3]$$

$$K_{3(900°C)} = 2.418x10^{-18} = \frac{a_{Na_2O(\ell)} \cdot P_{SO_3}}{a_{Na_2SO_4(\ell)}} \qquad [4]$$

For $a_{Na_2SO_4} = 0.844$ and assuming stoichiometric decomposition, the P_{SO_3} in the atmosphere is calculated to be $1.433x10^{-9}$ atm. The P_{SO_3} and P_{Cl_2} in the atmosphere above the Na_2SO_4-NaCl melt are also governed by the equilibrium conditions for the reaction

$$Na_2SO_4(\ell)+Cl_2(g) = 2NaCl(\ell) +SO_3(g)+\tfrac{1}{2}O_2(g) \qquad [5]$$

---

[1] R. H. Barkalow and F. S. Pettit in "High Temperature Metal Halide Chemistry," edited by D. L. Hildenbrand and D. D. Cubicciotti, Electrochemical Society, Princeton, N.J. (1978), p. 617.

[2] R. L. Jones and S. T. Gadomski, J. Electrochem. Soc., 124,1641, (1977).

$$K_{5(900°C)} = .0446 = \frac{(a_{NaCl(\ell)})^2 \ (P_{SO_3})(P_{O_2})^{\frac{1}{2}}}{a_{Na_2SO_4(\ell)} \cdot P_{Cl_2}} \qquad [C6]$$

For a_{NaCl} and $a_{Na_2SO_4}$ in the melt equal to 0.156 and 0.844 $\frac{P_{SO_3}}{P_{Cl_2}}$ respectively, and P_{O_2} equal to 0.21 atm. the equilibrium ratio is calculated to be 3.68. If $\frac{P_{SO_3}}{P_{Cl_2}}$ in the atmosphere is less than 3.68, Na_2SO_4 will be converted to NaCl. For a_{NaCl} and $a_{Na_2SO_4}$ in the melt equal to 0.156 and 0.844 respectively, stoichiometric decomposition gives P_{SO_3} and P_{Cl_2} of 1.433×10^{-9} atm. and 8.372×10^{-10} atm. respectively, and the $\frac{P_{SO_3}}{P_{Cl_2}}$ is 1.71, which is less than the equilibrium ratio $\frac{P_{SO_3}}{P_{Cl_2}}$. Thus, the Na_2SO_4 will be converted to NaCl. In the experiments of Barkalow and Pettit[1] and Jones et.al.[2], a continuous flow of NaCl(v) was maintained above the Na_2SO_4, thus Na_2SO_4 is continuously converted to NaCl. The vapor pressure of NaCl is high at 900°C (of the order of 2×10^{-3} atm), and under continuous flow conditions enhanced vaporization of Na_2SO_4 can be observed.

The enhanced vaporization of Na_2SO_4, due to the presence of NaCl, is more prominent as the temperature increases because of an increase in K_5 with temperature. Thermodynamic calculations indicate that the presence of NaCl alone can cause enchanced vaporization of Na_2SO_4 and formation of HCl(g), due to the reaction of NaCl with trace amount of H_2O in the furnace atmosphere, is not a necessary prerequisite for enhanced vaporization of Na_2SO_4, as has been indicated in the literature[3].

---

[3] C. A. Stearns, F. J. Kohl, G. C. Fryburg, and R. A. Miller in "High Temperature Metal Halide Chemistry," edited by D. L. Hildenbrand and D. D. Cubicciotti, Electrochem. Soc., Princeton, N.J. (1978) p. 555.

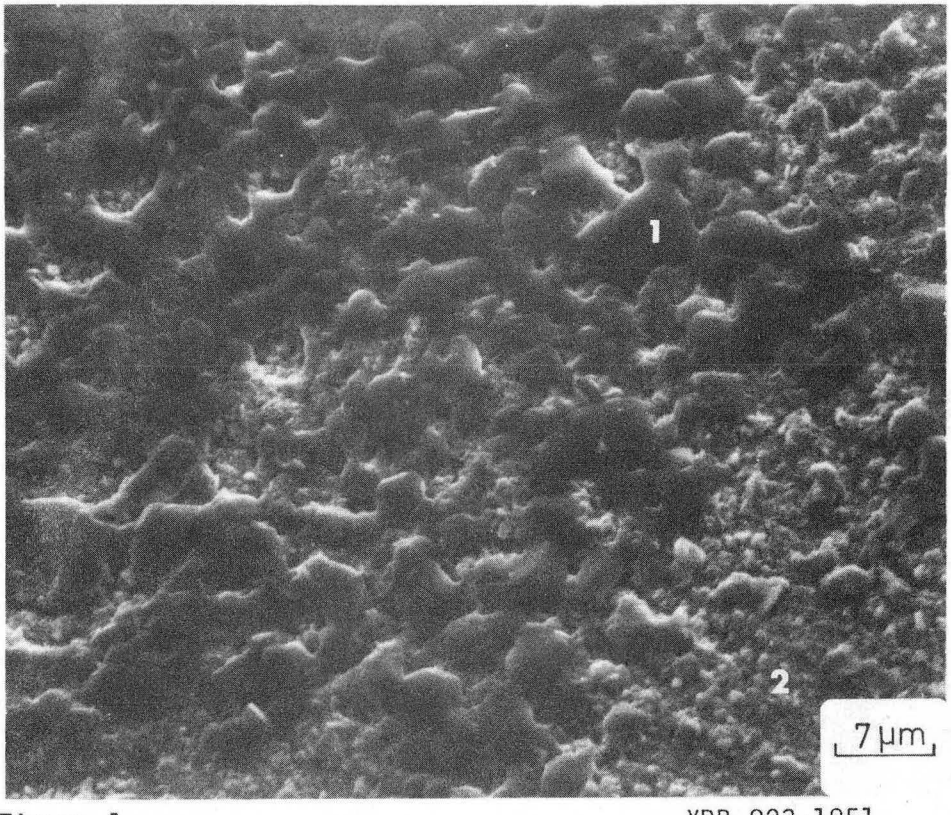

Figure 1 XBB 823-1851

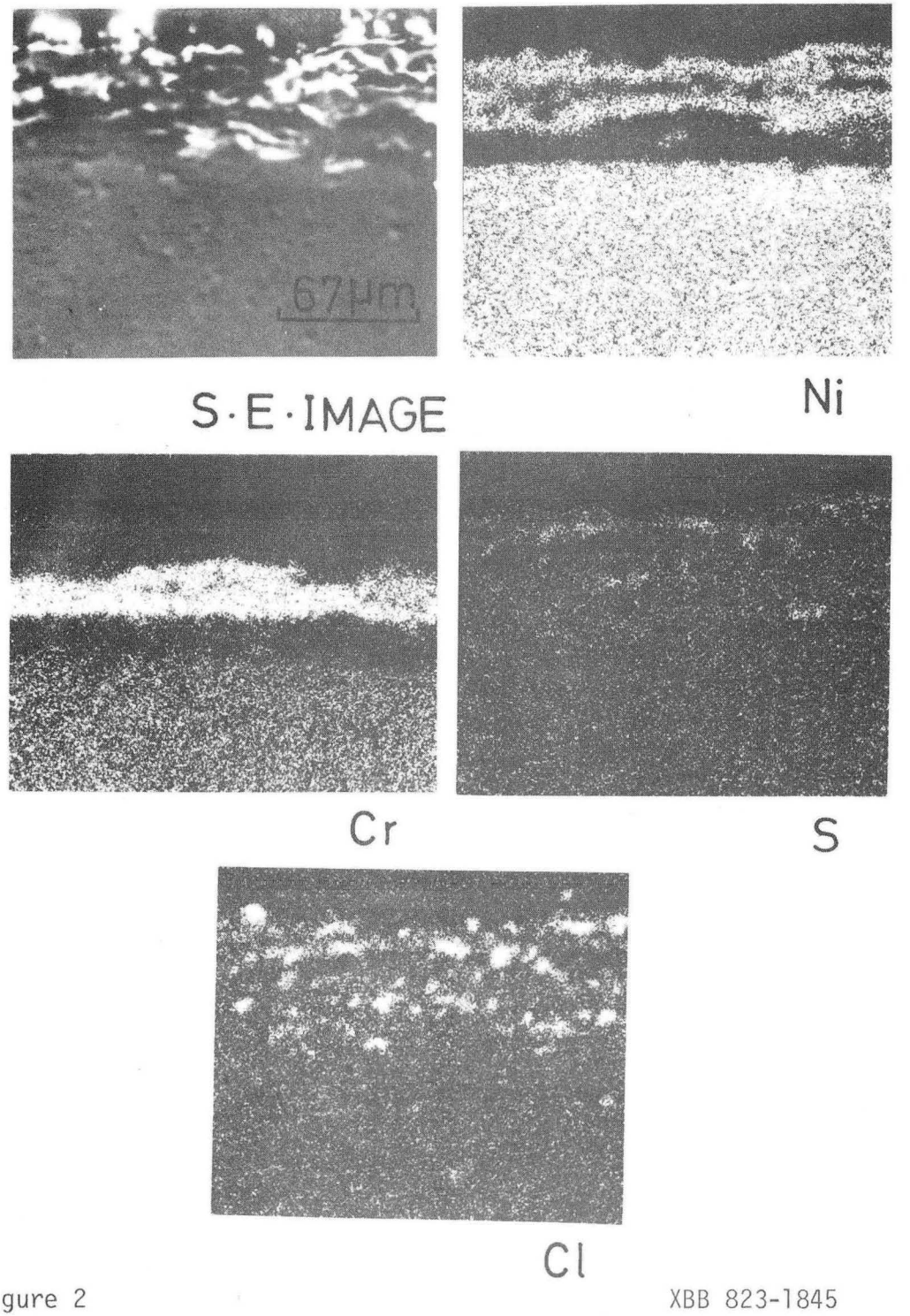

Figure 2

XBB 823-1845

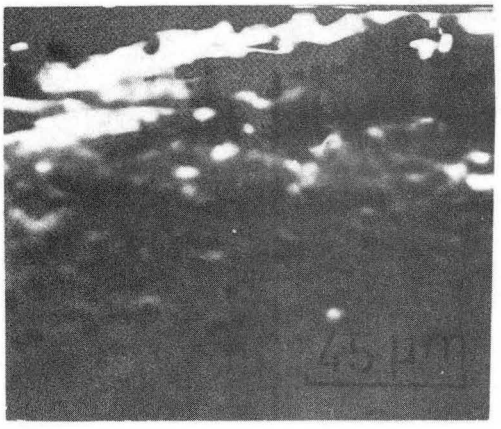

S·E·IMAGE

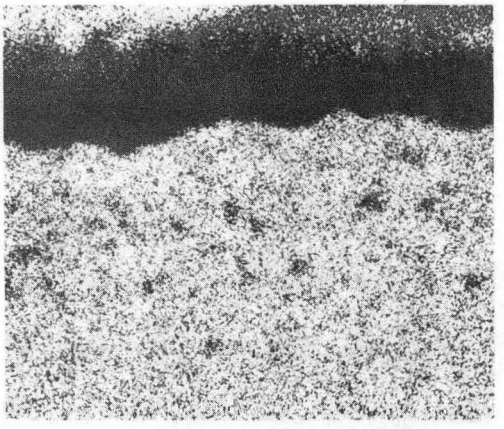

Ni

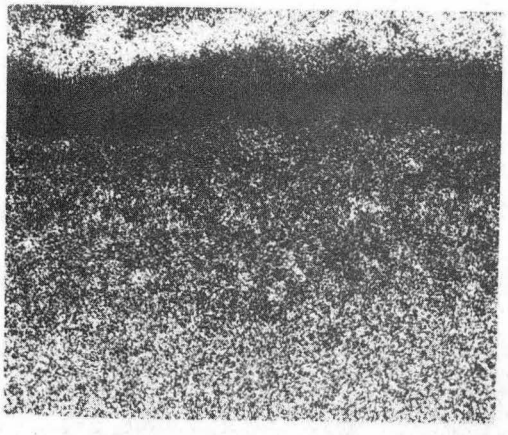

Cr

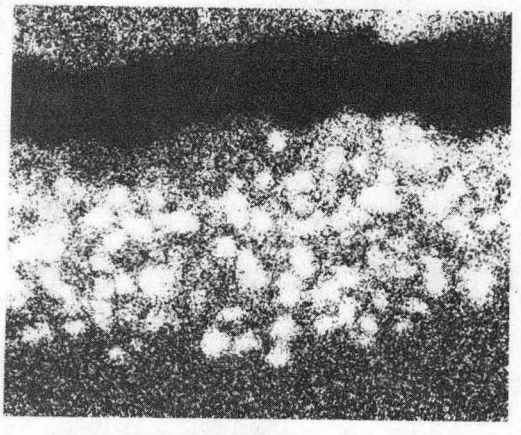

Cl

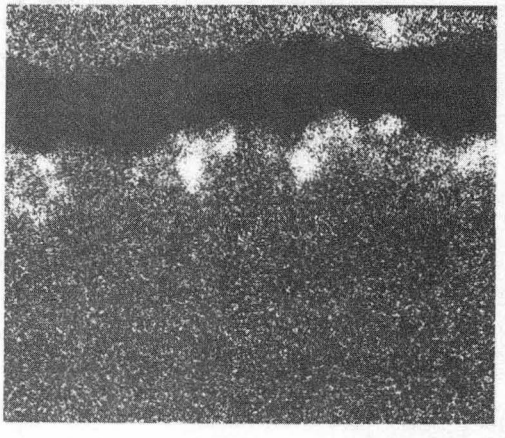

S

Figure 3

XBB 823-1850

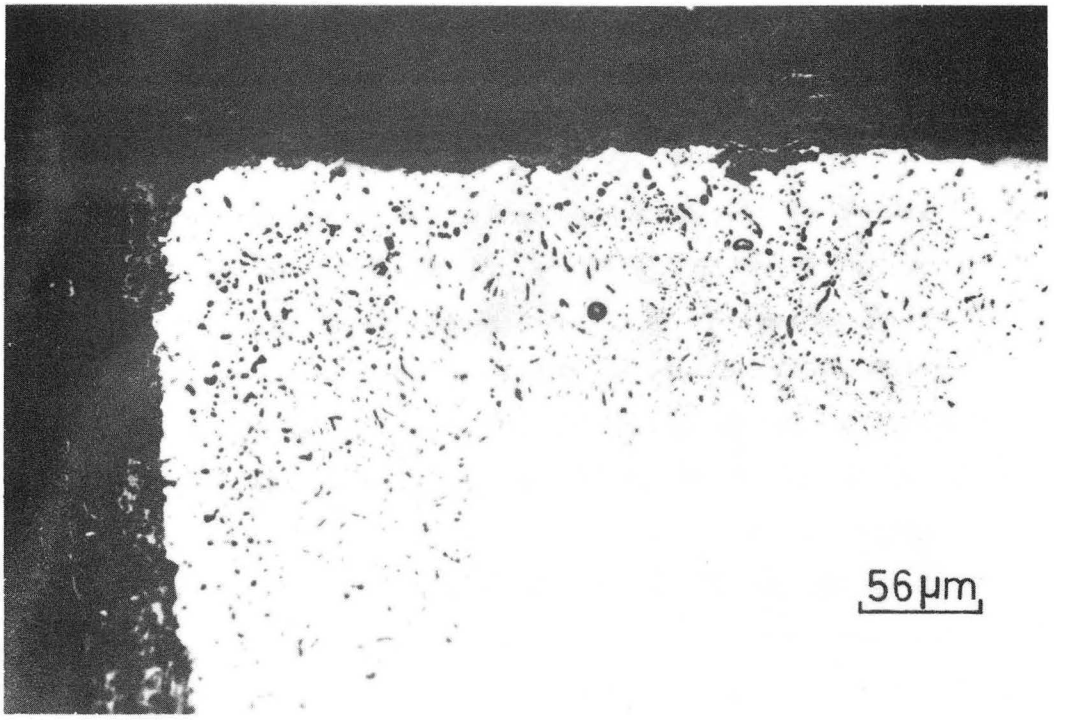

Figure 4

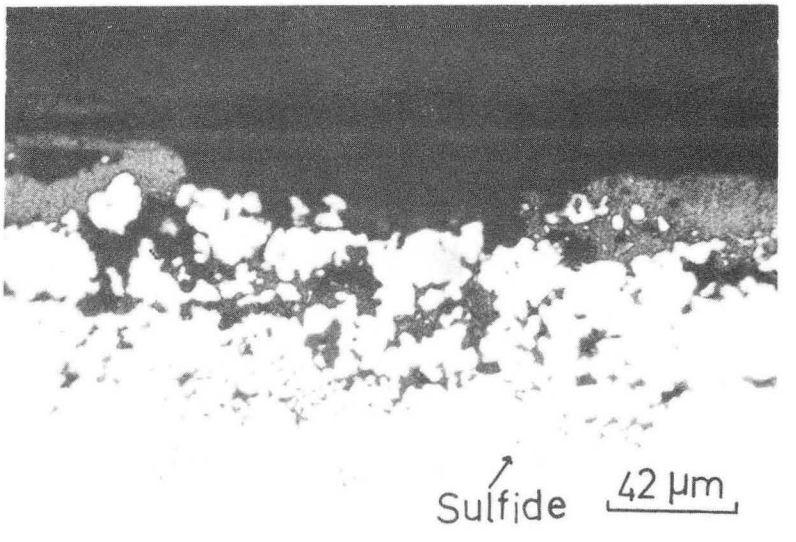

Figure 5

XBB 823-1846

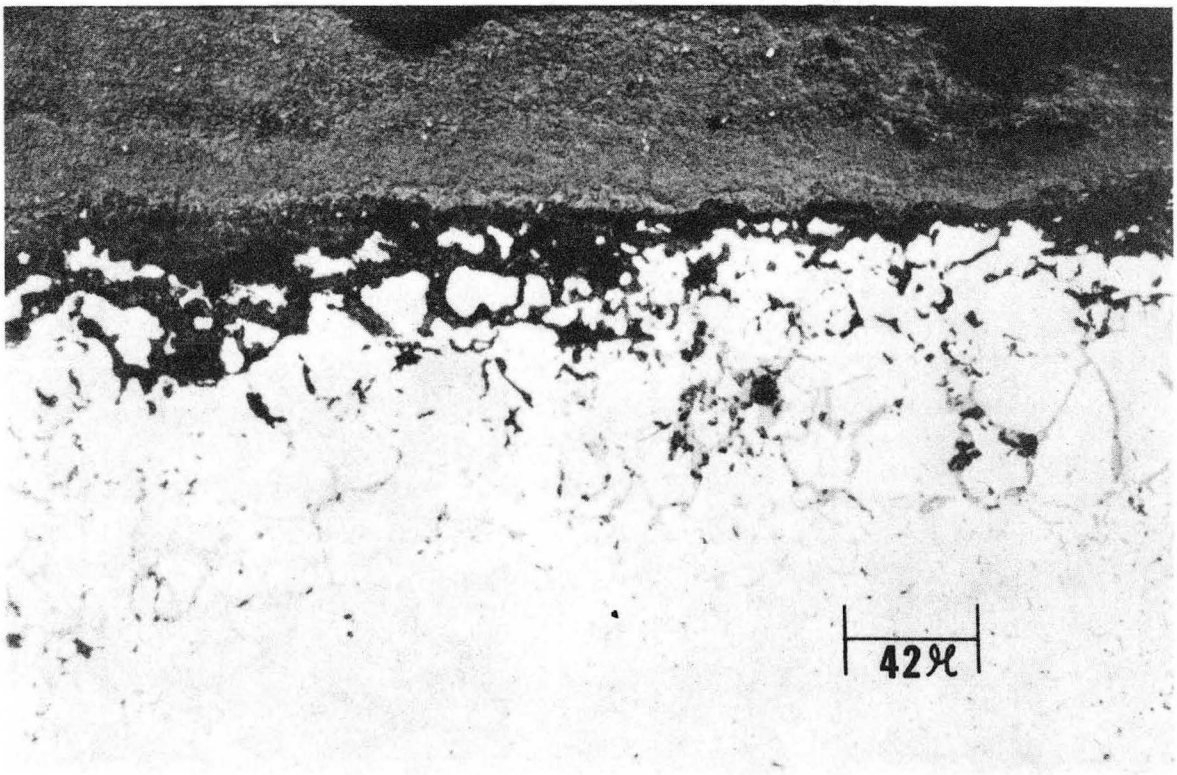

Figure 6

XBB 804-4161

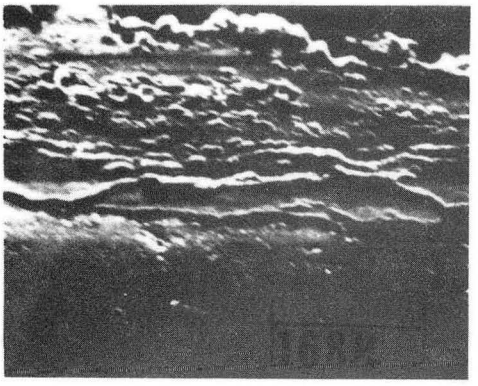

S.E.IMAGE

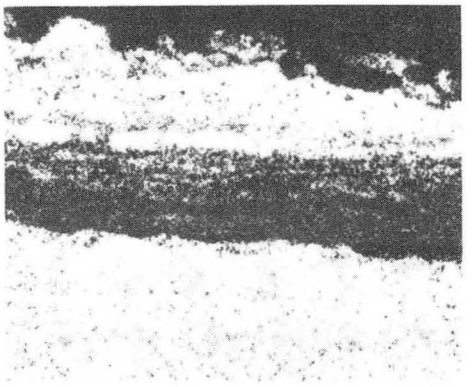

CO

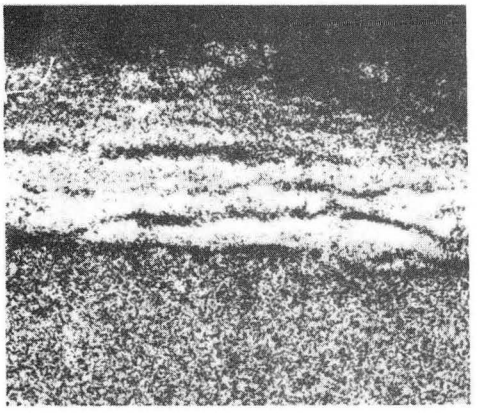

CR

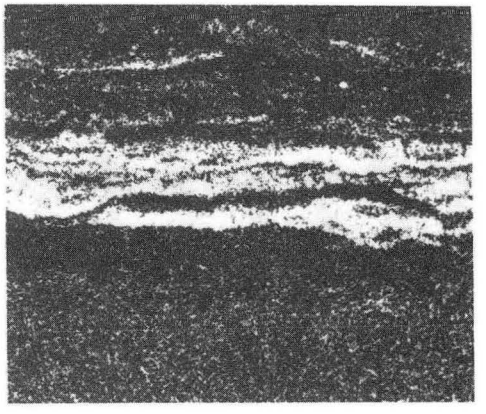

AL

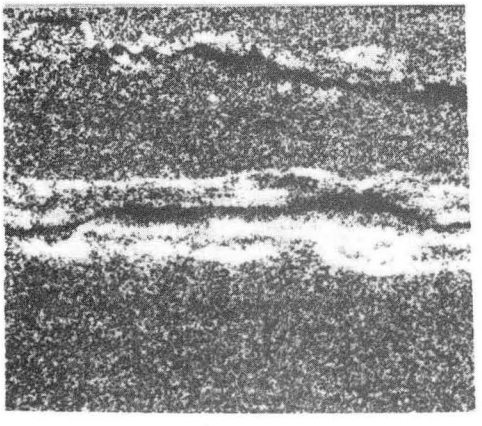

S

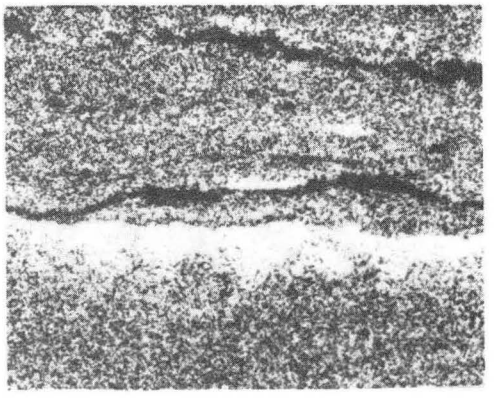

CL

Figure 7

XBB 804-4169

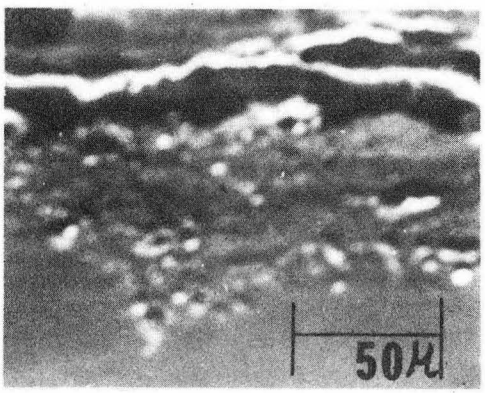

S.E.IMAGE

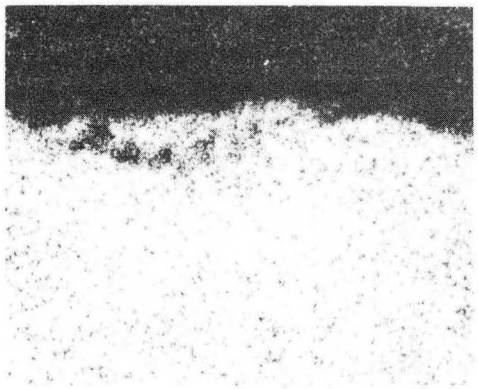

CO

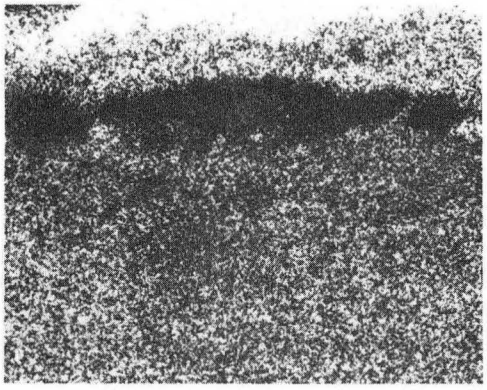

CR

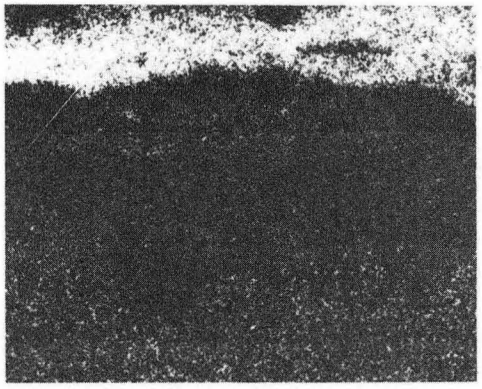

AL

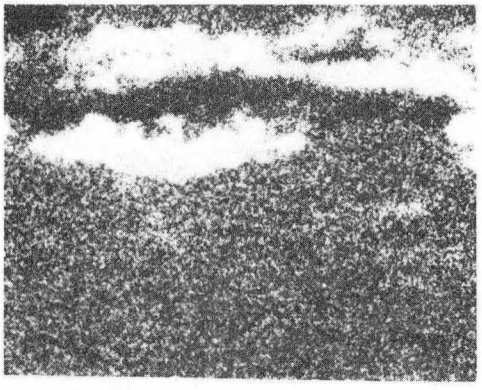

S

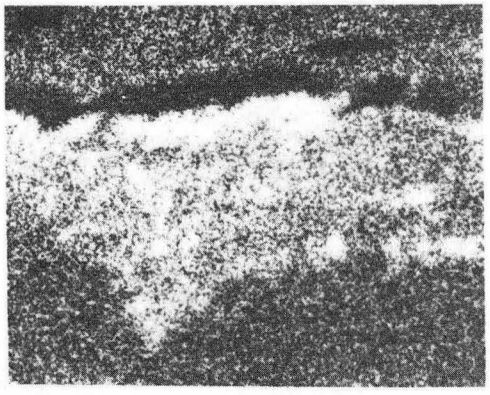

CL

Figure 8

XBB 804-4166

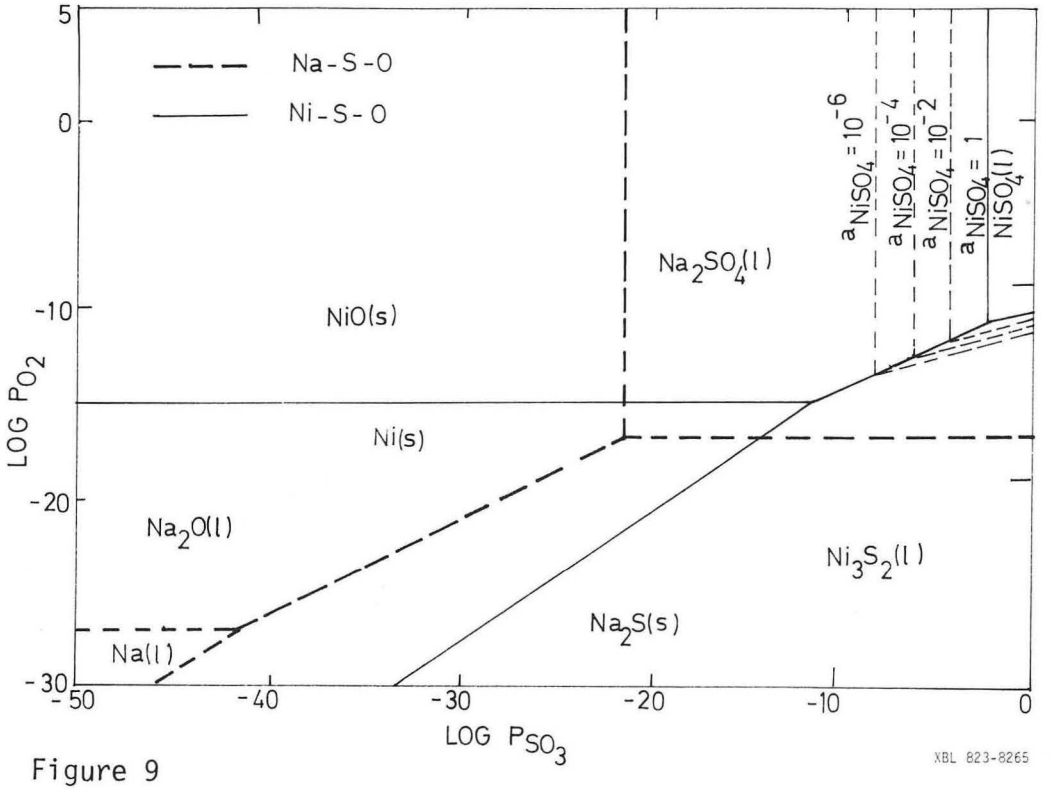
Na-S-O
Ni-S-O
$a_{NiSO_4}=10^{-6}$
$a_{NiSO_4}=10^{-4}$
$a_{NiSO_4}=10^{-2}$
$a_{NiSO_4}=1$
$NiSO_4(l)$
$Na_2SO_4(l)$
NiO(s)
Ni(s)
$Na_2O(l)$
$Ni_3S_2(l)$
$Na_2S(s)$
Na(l)
LOG P_{O_2}
LOG P_{SO_3}
5
0
-10
-20
-30
-50
-40
-30
-20
-10
0
XBL 823-8265

Figure 9

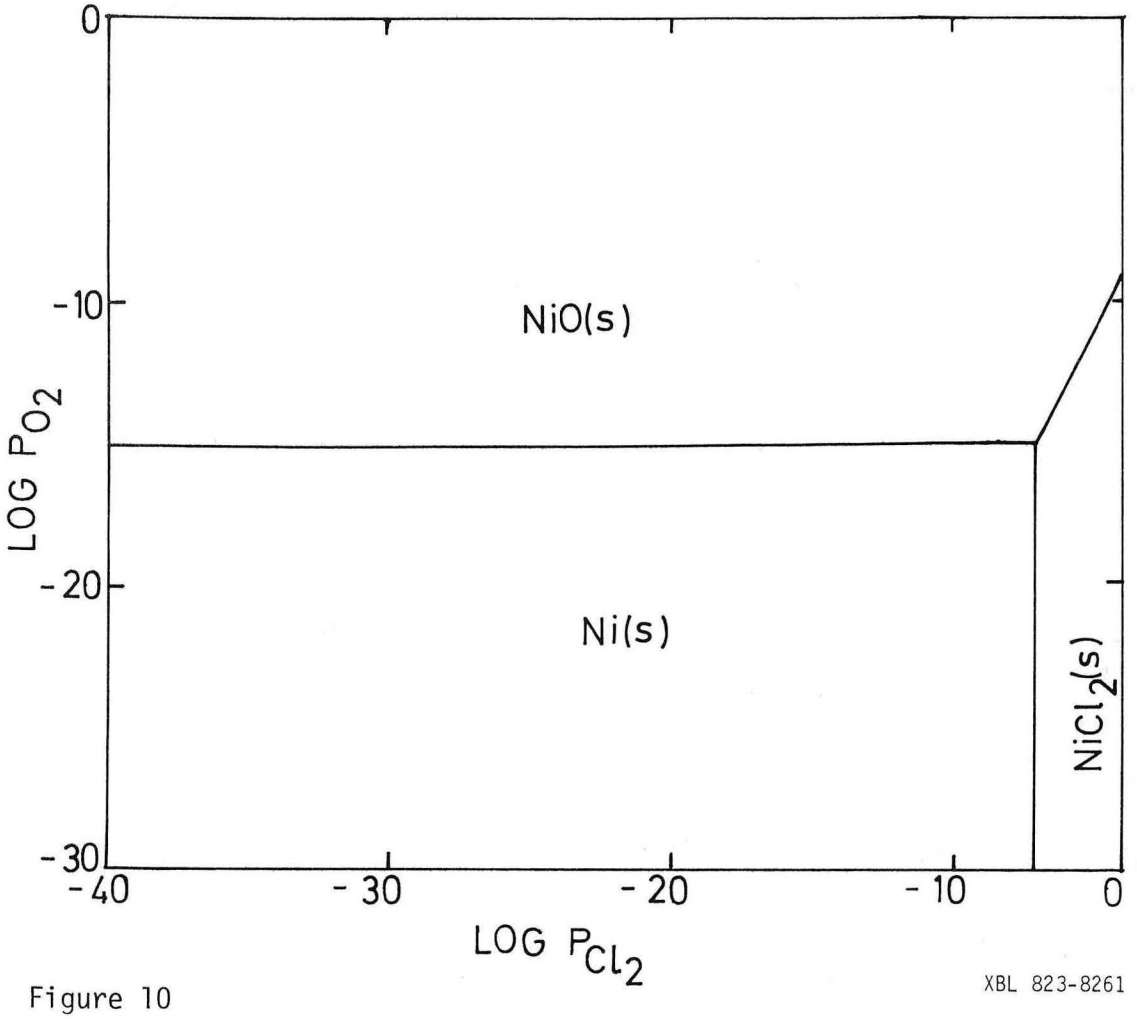

Figure 10

XBL 823-8261

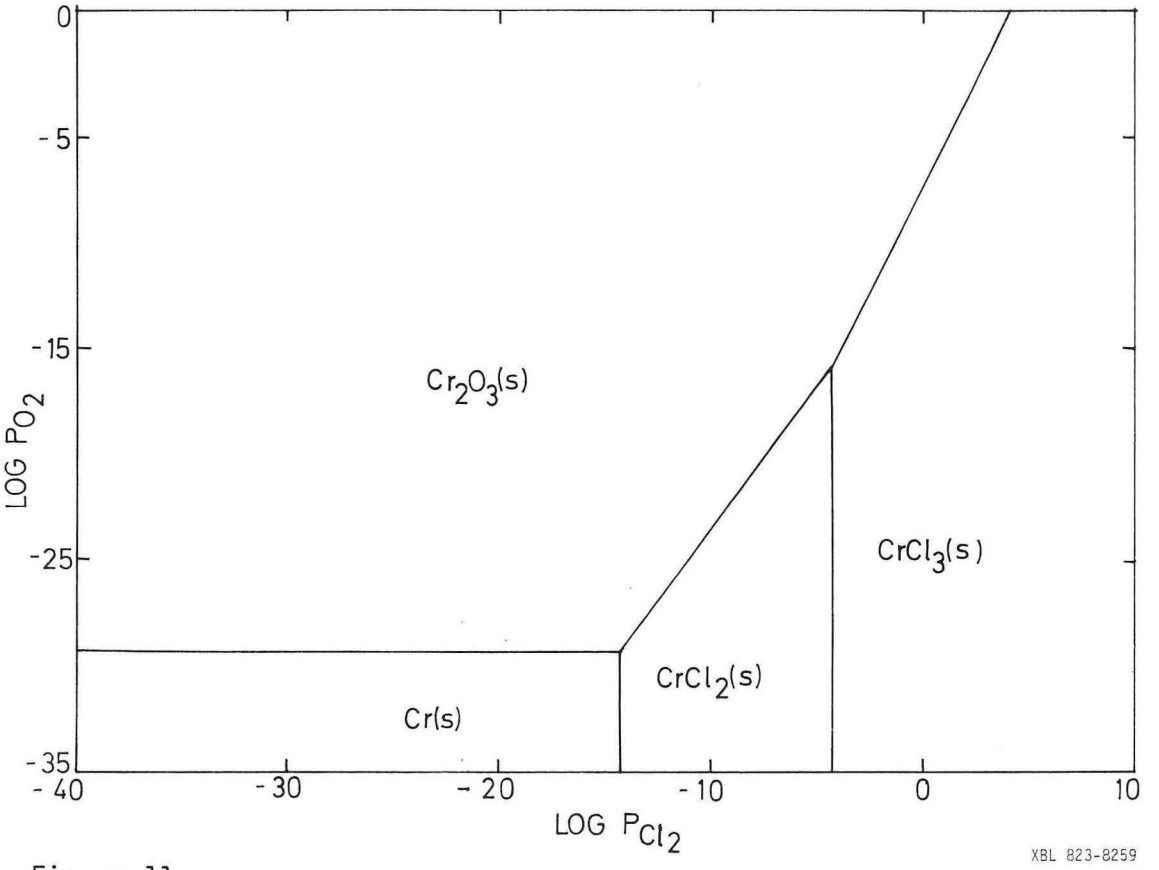
0
-5
-15
-25
-35
LOG P_{O_2}
$Cr_2O_3(s)$
$CrCl_3(s)$
$CrCl_2(s)$
Cr(s)
-40
-30
-20
-10
0
10
LOG P_{Cl_2}
XBL 823-8259

Figure 11

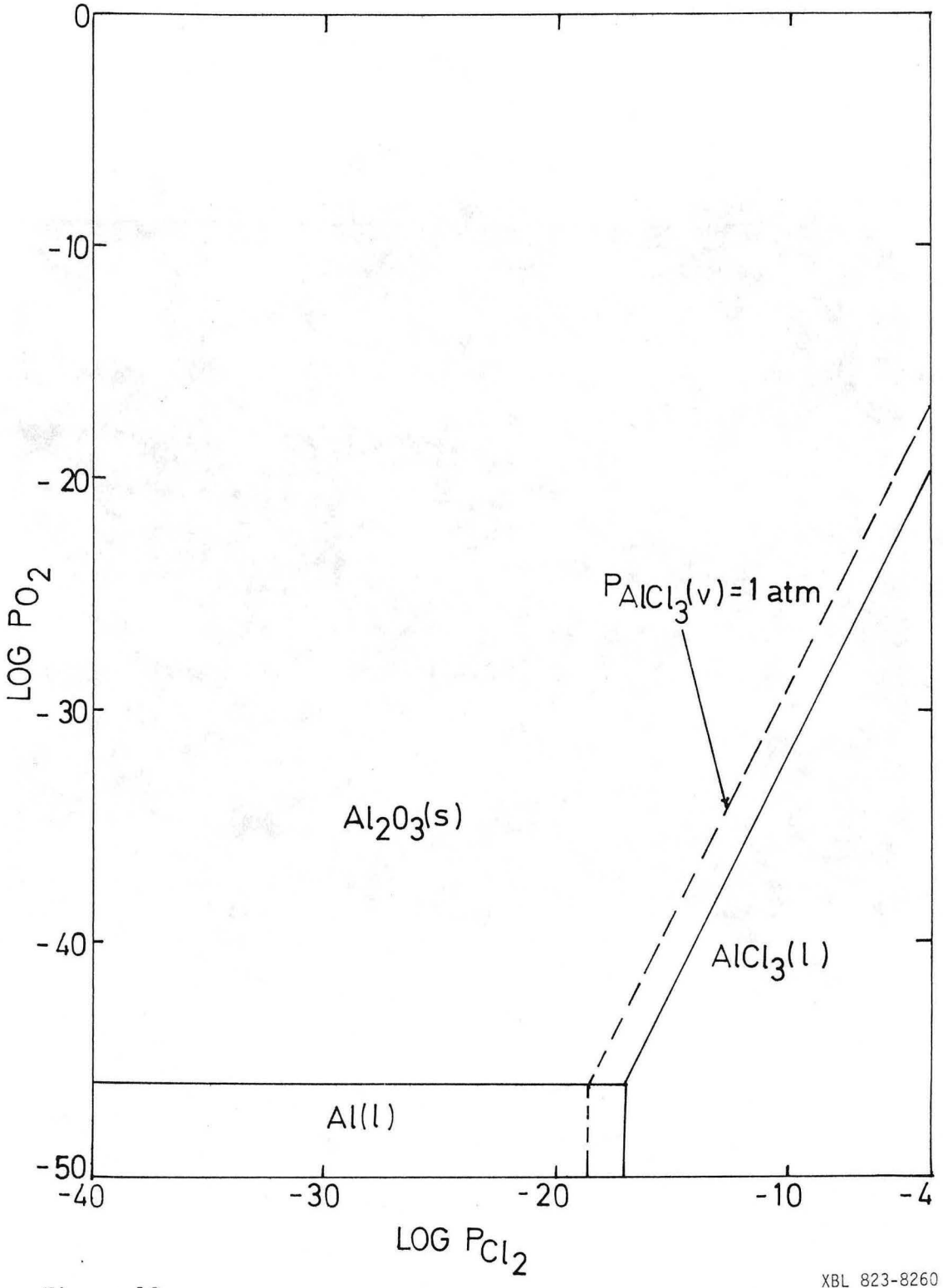

XBL 823-8260

Figure 12

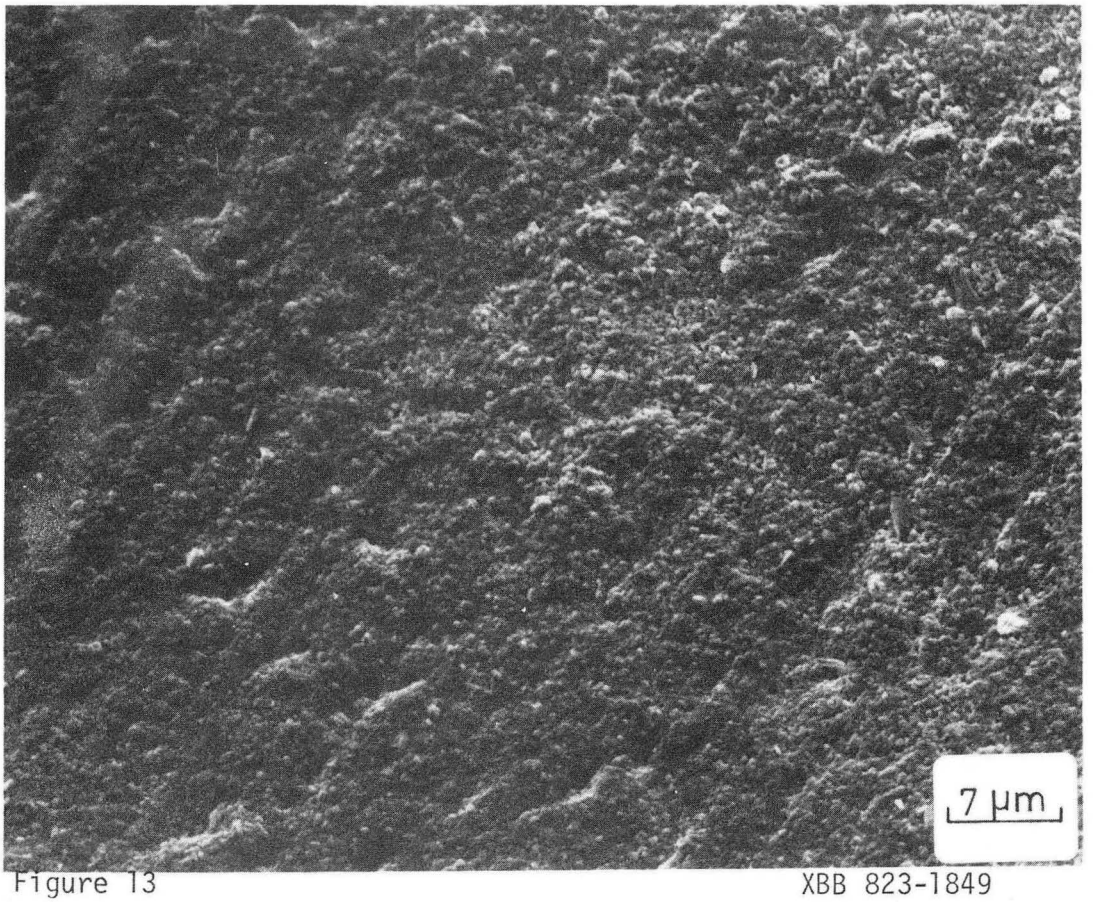

Figure 13 XBB 823-1849

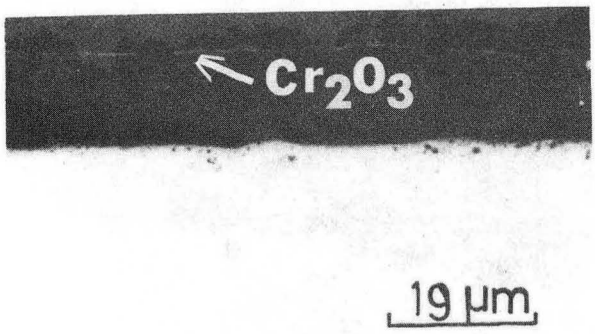

Figure 14

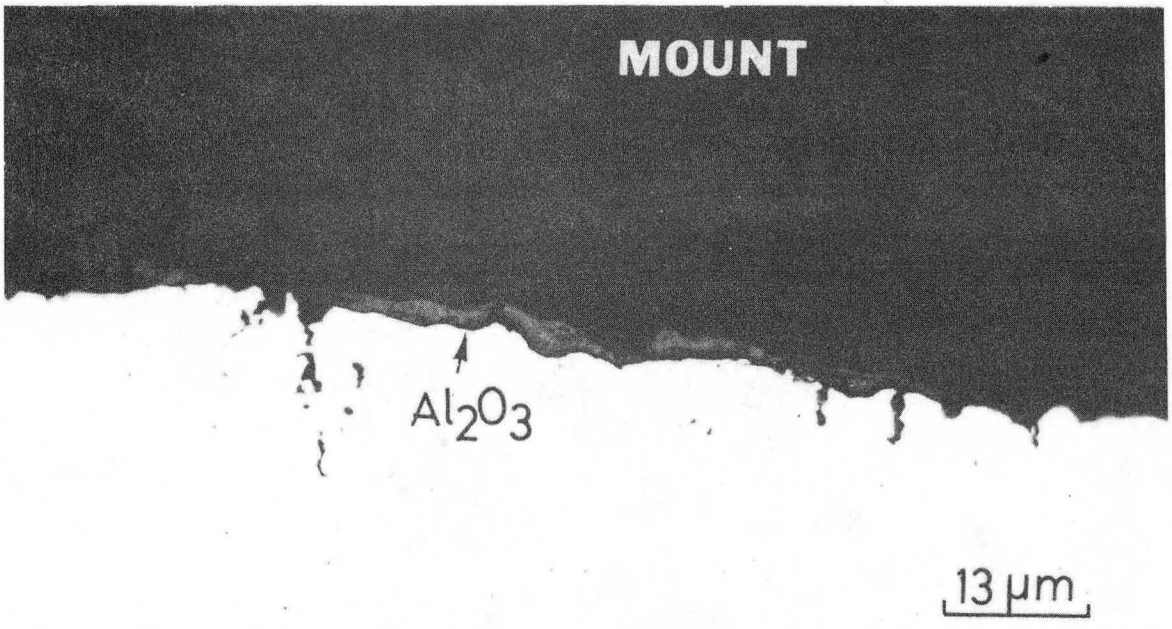

Figure 15

XBB 823-1848

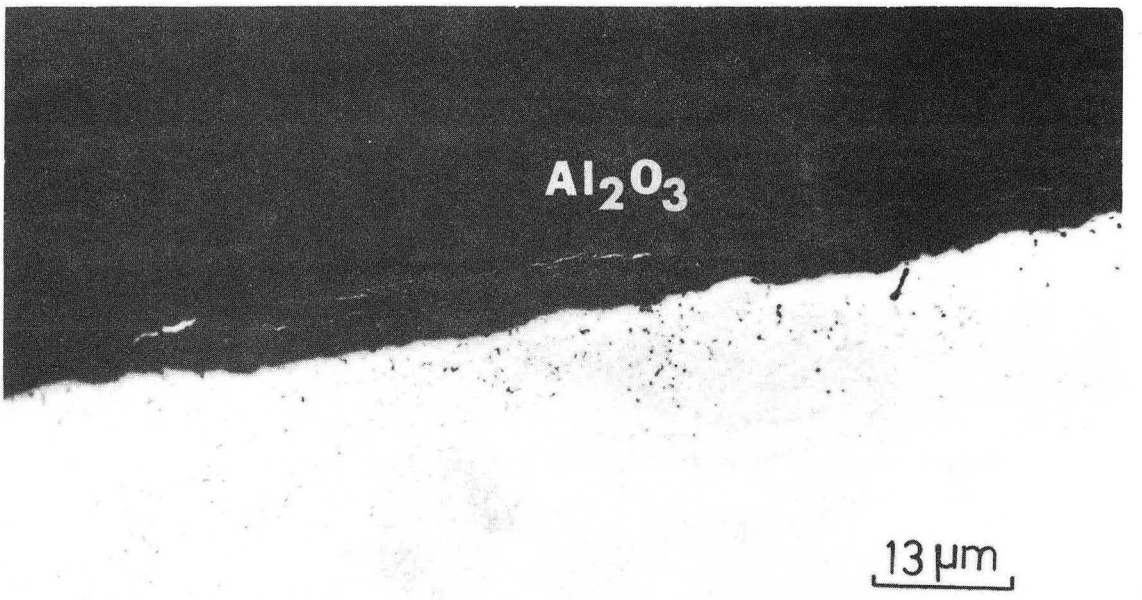

Figure 16

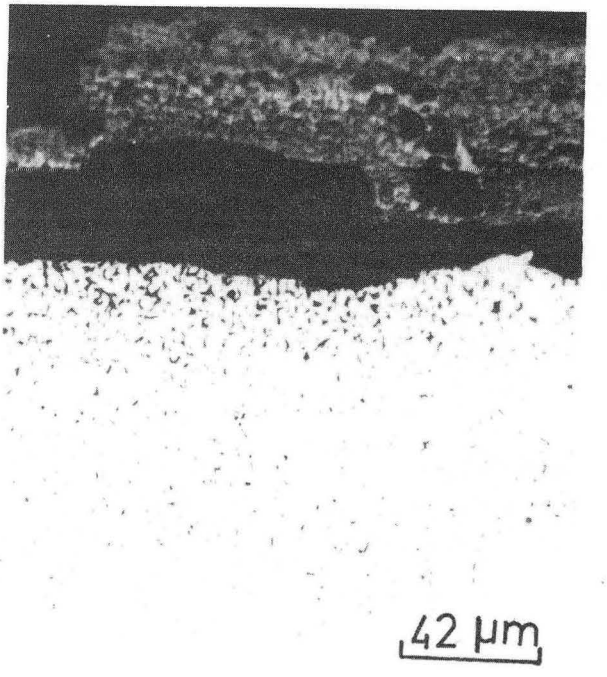

Figure 17

XBB 823-1847

TECHNICAL INFORMATION DEPARTMENT
LAWRENCE BERKELEY LABORATORY
UNIVERSITY OF CALIFORNIA
BERKELEY, CALIFORNIA 94720